

Self-adaption grey DBSCAN clustering

Shizhan Lu^{1*}

¹College of Economics and Management, Nanjing University of Science and Technology, Nanjing, 210094, China
(e-mail: lubolin2006@163.com)

Abstract

Clustering analysis, a classical issue in data mining, is widely used in various research areas. This article aims at proposing a self-adaption grey DBSCAN clustering (SAG-DBSCAN) algorithm. First, the grey relational matrix is used to obtain the grey local density indicator, and then this indicator is applied to make self-adapting noise identification for obtaining a dense subset of clustering dataset, finally, the DBSCAN which automatically selects parameters is utilized to cluster the dense subset. Several frequently-used datasets were used to demonstrate the performance and effectiveness of the proposed clustering algorithm and to compare the results with those of other state-of-the-art algorithms. The comprehensive comparisons indicate that our method has advantages over other compared methods.

Keywords: Clustering analysis, density-based, B-style grey relationship, SAG-DBSCAN.

1. Introduction

Cluster analysis, which focuses on the grouping and categorization of similar elements, is widely used in different research areas, such as climate predictions [1], gene expression [2], bioinformatics [3], finance and economics [4, 5], and neuroscience [6, 7].

In general, different clustering methods can be basically classified as follows: density-based (DP [8], DP-HD [9], DBSCAN [10], NQ-DBSCAN [11] and CSSub [12]); grid-based (CLIQUE [13], Gridwave [14] and WaveCluster [15]); model-based (Gaussian parsimonious [16], Gaussian mixture models [17] and Latent tree models[18]); partitioning (K-means [19, 20, 21], K-partitioning [22] and TLBO [23]); graph-based (SEGC [24], ProClust [25] and MCSSGC [26]); and hierarchical (BIRCH [27], K-d tree and Quadtree [28] and CHAMELEON [29]) approaches.

DBSCAN [10] is a representative density-based algorithm which clusters data by defining the density criterion with two parameters, Eps-distance and MinPts. NQ-DBSCAN [11], AA-DBSCAN [30], RNN-DBSCAN [31], ReCon-DBSCAN [32] and ReScale-DBSCAN [32] are some up-to-date developments of DBSCAN. As a disadvantage, DBSCAN and its extensions are difficult for their parameters to be set, which are ruleless on

account of the different densities for variant datasets.

Grey relational analysis is a significant tool for data mining [33, 34] and clustering analysis[35, 36, 37]. In this article, grey relational analysis is applied to obtain grey local density indicator for every object in clustering dataset. And then, grey local density indicator is applied to make noise identification for obtaining a dense subset. The dense subset which the border points of i th cluster are far away from the border points of j th cluster is easily to set parameters for DBSCAN. This method overcomes the disadvantage of DBSCAN which is difficult for its parameters to be set for variant datasets.

The remainder of this article is organized as follows: Section 2 presents a grey local density indicator, proposes a method for self-adaption noise identification and proposes a self-adaption grey-DBSCAN clustering method. Section 3 demonstrates our algorithms by some numerical experiments of both simulated and real datasets and make comparisons with the state-of-the-art clustering algorithms. Section 4 gives a conclusion.

2. Proposed methods

The main framework of the SAG-DBSCAN algorithm can be described as follows. Step 1 obtains the matrix of the B-style grey relationship degree and grey local density indicator ρ . Step 2 utilizes linear regression to obtain dense subset C (as shown in Fig. 1 (b)). Step 3 applies DBSCAN algorithm to cluster dense subset (as shown in Fig. 1 (c)). Step 4 assigns the object in $X - C$ to its nearest cluster (as shown in Fig. 1 (d)).

2.1. Grey local density indicator

For all $x_i = (x_i(1), x_i(2), \dots, x_i(N))$ and $x_j = (x_j(1), x_j(2), \dots, x_j(N))$ in N -dimensional dataset X ,

$$\gamma(x_i, x_j) = \frac{1}{1 + d_{ij}^{(0)}/N + d_{ij}^{(1)}/(N-1) + d_{ij}^{(2)}/(N-2)} \quad (1)$$

is the B-style grey relationship degree of x_i and x_j [38, 39], where $d_{ij}^{(0)} = \sum_{k=1}^N |x_i(k) - x_j(k)|$, $d_{ij}^{(1)} =$

$$\sum_{k=1}^{N-1} |x_i(k+1) - x_j(k+1) - x_i(k) + x_j(k)| \text{ and } d_{ij}^{(2)} = \sum_{k=2}^{N-1} |x_i(k+1) - x_j(k+1) - 2(x_i(k) - x_j(k)) + x_i(k-1) - x_j(k-1)|. G = [\gamma(x_i, x_j)]_{n \times n}$$
 is denoted as B-style grey relationship degree matrix.

B-style grey relationship degree is superior to other grey relationship degrees and Euclidean distance function for describing the objects' relationships about object displacement, such as the DrivFace dataset in our experiments. Meanwhile, it can work well for other simulated data (Euclidean space points) like Euclidean distance function. B-style grey relationship degree has strong applicability and generality for various datasets, hence, it is selected to make following analysis.

KNN-density is a frequently-used indicator to describe the local density indicator ρ_i [40, 41]. A relatively straightforward and useful grey KNN-density indicator is projected as equation (2), where $|GKNN(x_i)| = k$ and $G(i, j) \geq G(i, t)$ for all $x_j \in GKNN(x_i)$ and $x_t \in X - GKNN(x_i)$.

$$\rho_i = \sum_{x_j \in GKNN(x_i)} G(i, j), \quad (2)$$

In general, the dense family of a cluster is composed of many objects with large grey relationship degree between each other, on the contrary, the border objects has small grey relationship degree with its neighbors. As shown in Fig. 1 (c), the dense subset C is composed of many dense families C_i ($1 \leq i \leq t$). The object x_j of dense family has a large value of ρ_j via calculating by equation (2) if we set $k \leq \min\{|C_i| : i = 1, 2, \dots, t\}$, where C_i is the dense family of i th cluster.

2.2. Self-adaption method for noise identification

Data preprocessing is necessary for the grey local density indicator ρ before the noise identification. Let $\rho' = \{\rho'_i : 1 \leq i \leq n\}$ be the descending sequence of $\rho = \{\rho_j : 1 \leq j \leq n\}$ and $V = \{v_i : 5 \leq i \leq n\}$ be the mean smoothing sequence of ρ' , where $v_i = (\rho'_i + \rho'_{i-1} + \rho'_{i-2} + \rho'_{i-3} + \rho'_{i-4})/5$.

As shown in Fig. 2, the elements of V have two distinctly different distribution trends. The elements in V are divided into two parts $V_p^- = \{v_i : 5 \leq i \leq p\}$ and $V_p^+ = \{v_i : p < i \leq n\}$ for linear regression, and f_1 and f_2 are the regression equations for V_p^- and V_p^+ , respectively.

$$\begin{cases} e_1(i) = f_1(i) - v_i, 5 \leq i \leq p, \\ e_2(i) = f_2(i) - v_i, p < i \leq n. \end{cases} \quad (3)$$

$R = \sum_{5 \leq i \leq p} |e_1(i)| + \sum_{p < i \leq n} |e_2(i)|$ is the regression residual.

As shown in Fig. 2, we pick p_1, p_2 and p_3 in different positions for linear regressions and obtain three regression residuals R_1, R_2 and R_3 , where f_1 and f_2 are the regression straight line with respect to $V_{p_2}^-$ and $V_{p_2}^+$, respectively. The results show that $R_2 < R_1$ and $R_2 < R_3$.

After investigating the characteristic of the grey local density indicator ρ and the smoothing sequence V , we can make a sequence of linear regressions to obtain a residual sequence $R = \{R_i : 5 + 5 \leq i \leq n - 5\}$ (5 points for regression). If $R_p = \min(R)$, the object x_j is considered as a member of dense subset for the case $\rho_j \geq \rho'_p$. Then, the dense subset (as shown in Fig. 1 (c)) is obtained for clustering by DBSCAN method.

2.3. Self-adaption grey DBSCAN clustering method (SAG-DBSCAN)

The detailed processes of the SAG-DBSCAN algorithm are shown as Algorithm 1.

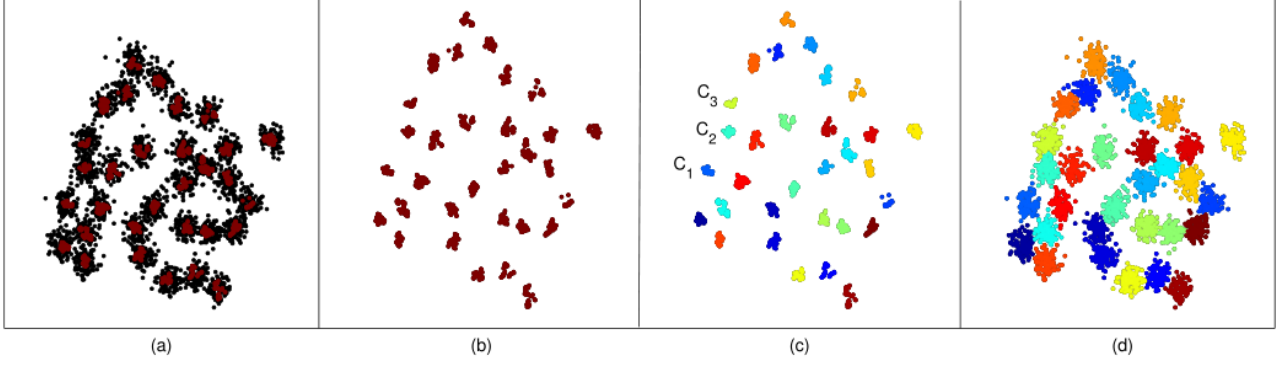


Figure 1: The main framework of the SAG-DBSCAN algorithm

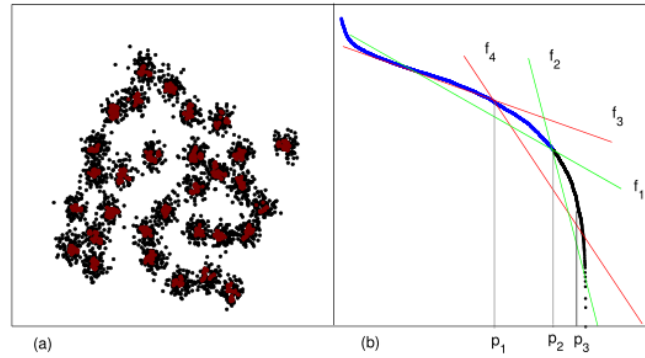


Figure 2: The distinctions of border points and dense area points showed in V

Algorithm 1: SAG-DBSCAN algorithm.

Input: Dataset, parameters $k \in N^+$ and $m \in N^+$.

Output: The clustering result.

1. Use equation (1) to obtain B-style grey relationship degree matrix G .
 2. Apply equation (2) to obtain grey local density indicator ρ with respect to $k = |GKNN(x_i)|$.
 3. Sort ρ to obtain ρ' , smooth ρ' to obtain V .
 4. Obtain dense subset $C \subset X$ by linear regression of V .
 5. Set $\text{MinPts}=m$ and $\text{Eps-distance}=\max\{d(x_i, x_i^{(m)}) \mid x_i \in C\}$, where $x_i^{(m)}$ is the m th neighbor of x_i .
 6. Apply DBSCAN to cluster dense subset C with $\text{MinPts}=m$ and Eps-distance .
 7. Assign the objects of $X - C$ to their nearest clusters.
-

The objects of $X - C$ can be assigned as follows: let $A \subset X$ be the subset that contains the already classified points and $U \subset X$ be the subset of unclassified points. If $f(x'_i, x'_j) = \min\{f(x_i, x_j) : x_i \in A, x_j \in U\}$, then x'_j is assigned to the category that contains x'_i .

The time complexities are $\mathcal{O}(n^2)$ and $\mathcal{O}(n)$ for obtaining B-style grey relationship degree matrix G and dense subset C , respectively. The time complexity of DBSCAN is $\mathcal{O}(n^2)$ at the worst case. Moreover, if $|C| = n'$, then $|X - C| = n - n'$, and the time complexity of assigning border points is hence $\mathcal{O}(n - n')$.

3. Experiments

In this section, we evaluate the performance and effectiveness of the proposed method on both simulation data and real data, and then compare it with some up to date methods: the affinity propagation algorithm (AP) [42], automatic find of density peaks (ADPC)

Dataset	Instances	Features	Clusters	Dataset	Instances	Features	Clusters	Detail
D31	3100	2	31	Iris	150	4	3	three kinds of irises: Setosa, Versicolour and Virginica. Each kind has 50 samples
S1	5000	2	15	Wifi	2000	7	4	2000 times of signal records in 4 rooms, 500 records in each room
R15	600	2	15	Vertebral	310	6	2	310 orthopaedic samples, 210 abnormal samples and 100 normal samples
Dim2	1350	2	9	TumTyp	801	20531	5	gene expressions of patients having different types of tumor: BRCA, KIRC, COAD, LUAD and PRAD.
ShapeT	10000	2	3	DrivFace	606	6400	4	dataset contains images sequences of subjects while driving in real scenarios. It is composed of 606 samples and acquired over different days from 4 drivers with several facial features.

Table 1: The simple description of datasets

[43], Neighbor Query DBSCAN (NQ-DBSCAN) [11] and NK hybrid genetic algorithm (NKGa) [44].

3.1. Descriptions of Experiment data

First, some frequently-used datasets obtained from different references are used to test the algorithms, such as R15 [45], D31 [45], S1 [46] and Dim2 [47] etc. And then a dataset, ShapeT (Fig. 3), is constructed for the supplementary tests. All the simulation data are points of two-dimensional Euclidean space.

Several real-world datasets are used to test the performance of the proposed method, including a plant dataset: Iris [48, 49]; a wireless signal dataset: Wifi [50]; a human vertebral column dataset: Vertebral [51]; a gene dataset: TumTyp [52]; and a face image dataset: DrivFace [53]. Datasets were taken from the UCI¹ repository. Simple descriptions of these real datasets are provided in Table 1.

3.2. Results and Comparisons

3.2.1. Results presentation

Table 2 presents the number of clusters estimated by different methods. Table 3 shows the clustering results when compared with other methods.

To evaluate and compare the performance of the clustering methods, we apply the evaluation metrics: Accuracy, F-Score, Adjusted Rand Index (ARI) [54] and Normalized Mutual Information (NMI) [55] in our experiments to do a comprehensive evaluation. The higher the value, the better the clustering performance for all these measures. Compared with the best results of other algorithms, our method has relative advantages of 0.0936, 0.3938, 0.0535 and 0.1494 (TABLE 3)

with respect to Accuracy, F-Score, ARI and NMI for the Vertebral dataset, respectively.

We conduct the Friedman test with the post-hoc Nemenyi test [12] to examine whether the difference between any two clustering algorithms is significant in terms of their average ranks. The difference between two algorithms is significant if the gap between their ranks is larger than CD. There is a line between two algorithms if the rank gap between them is smaller than CD. This test shows that SAG-DBSCAN, ADPC and NQ-DBSCAN are significantly better than NKGa and AP. SAG-DBSCAN is the best performer of these algorithms, followed by ADPC (as shown in Fig. 4).

In summary, our method obtains better results with respect to the estimation of cluster number, Accuracy, F-Score, ARI and NMI, compared comprehensively with other methods.

3.2.2. Parameter analysis

The parameters of the proposed method can be set with a reference of the number of objects in clustering dataset X . For these datasets, we set $m = 3$ when $n < 500$, $m = 4$ when $500 \leq n < 1000$, $m = 5$ when $1000 \leq n < 5000$ and $m = 10$ when $n \geq 5000$. We set $k = \text{ceil}(2\%n)$ when $n < 1000$, $k = \text{ceil}(1\%n)$ when $1000 \leq n < 2000$ and $k = 20$ when $n \geq 2000$.

The parameters of NQ-DBSCAN are shown in Table 4, for example Eps-distance=0.6 (left) and MinPts=23 (right) for D31 dataset. The parameter settings of NQ-DBSCAN are random and ruleless for the datasets. It is thus difficult to guess the right parameters for NQ-DBSCAN if the results are unknown before clustering occurs.

¹<http://archive.ics.uci.edu/ml/datasets.php>

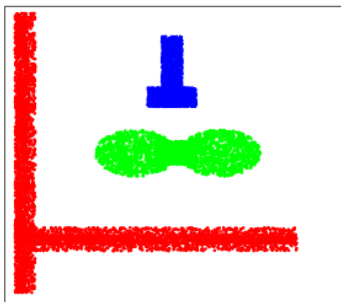


Figure 3: ShapeT

Dataset	The estimated number of clusters					Dataset	The estimated number of clusters				
	AP	ADPC	NKGA	NQ-DBSCAN	SAG-DBSCAN		AP	ADPC	NKGA	NQ-DBSCAN	SAG-DBSCAN
D31	8	31	19	31	31	Iris	2	2	11	3	3
S1	15	15	14	15	15	Wifi	5	4	1	4	4
R15	5	15	15	15	15	Vertebral	1	1	2	2	2
Dim2	7	9	9	9	9	TumTyp	3	5	6	5	5
ShapeT	27	5	11	3	3	DrivFace	5	6	3	5	4

Table 2: Number of clusters estimated by various methods

D31	S1	R15	Dim2	ShapeT
0.6, 23	5000, 19	0.3, 6	5000, 10	0.2746, 10
Iris	Wifi	Vertebral	TumTyp	DrivFace
0.42, 5	6, 20	16, 7	166.05, 5	10.26, 5

Table 4: The parameter settings of NQ-DBSCAN

The proposed method is robust. It can obtain the same clustering result when we select values for parameters k and m at wide intervals. For example, SAG-DBSCAN can obtain the same results for dataset Iris with $k \in [5, 11] \cap N^+$ when $m = 3$. For dataset Iris, NQ-DBSCAN cannot obtain the same results for three cases; Eps=0.41, Eps=0.42 and Eps=0.43, when MinPts=5. NQ-DBSCAN is not robust in their parameters.

The parameter of ADPC [43] is set with $d_c = 0.02$ for these datasets. $d_c = 0.02$ means that the parameter of ADPC takes the value at the position of first 2% of all distances [43].

3.2.3. Comparisons and discussions

AP [42] is an unsupervised algorithm without any parameters. The parameters of NKGA [44] are recommended by the publication [44]. The algorithms of parameter-free or fixed parameter value may not be adaptive to various kinds of datasets.

ADPC can obtain good results in most instances. However, as a centroid-based method, ADPC and its variants cannot cluster objects correctly when a category has more than one center, such as the ShapeT

dataset which has no single point can be considered as the geometrical centroid of the T shape cluster.

The NQ-DBSCAN produces good results for two-dimensional data after it tunes the parameters many times with reference to two-dimensional figures. However, it does not work well for high-dimensional data, because these data cannot show well in two-dimensional figures. It is hampered by the ruleless parameters when it deals with multidimensional data. SAG-DBSCAN sets its parameters according to the number of objects, it is easier to set parameters than NQ-DBSCAN. SAG-DBSCAN obtains better results more easily than NQ-DBSCAN do, when faced with a new high-dimensional dataset that has no references to known clustering results.

4. Conclusion

In this article, the SAG-DBSCAN algorithm is proposed, and then some simulation and real data are used to test the performance and effectiveness of the proposed method. Moreover, our proposed algorithm is also compared with several frequently-used clustering algorithms, including the intelligent algorithm NKGA, the centroid-based algorithm ADPC, the parameter-free self-adaption algorithm AP and an improved DBSCAN algorithm NQ-DBSCAN. The experiments indicate that our method obtains better results, in terms of the evaluation metrics (TABLE 3) and the estimated

Dataset	Measures	AP	ADPC	NKGA	NQ-DBSCAN	SAG-DBSCAN	Dataset	Measures	AP	ADPC	NKGA	NQ-DBSCAN	SAG-DBSCAN
D31	Accuracy	0.2210	0.9677	0.3539	0.5416	0.9677	Iris	Accuracy	0.5333	0.6667	0.4533	0.7867	0.9067
	F-Score	0.3466	0.9679	0.4537	0.6937	0.9679		F-Score	0.4329	0.5714	0.5883	0.8697	0.9168
	ARI	0.1704	0.9352	0.3290	0.1240	0.9352		ARI	0.4120	0.5681	0.2681	0.6789	0.7592
	NMI	0.4929	0.9573	0.6498	0.2994	0.9573		NMI	0.4509	0.7337	0.0138	0.7603	0.8057
S1	Accuracy	0.7642	0.9262	0.6992	0.9614	0.9932	Wifi	Accuracy	0.1405	0.8625	0.2500	0.7545	0.9355
	F-Score	0.7907	0.9332	0.7315	0.9647	0.9934		F-Score	0.1671	0.8859	0.1000	0.8561	0.9402
	ARI	0.6518	0.8915	0.5685	0.9378	0.9858		ARI	0.1948	0.8103	0.0000	0.6868	0.8470
	NMI	0.8382	0.9450	0.7878	0.9695	0.9895		NMI	0.2646	0.8309	0.0078	0.6531	0.8635
R15	Accuracy	0.2217	0.9917	0.8983	0.8200	0.9933	Vertebral	Accuracy	0.6774	0.6774	0.6645	0.1516	0.7710
	F-Score	0.3416	0.9918	0.9035	0.9011	0.9935		F-Score	0.4038	0.4038	0.3992	0.1437	0.7976
	ARI	0.2574	0.9817	0.7968	0.7667	0.9857		ARI	0.0335	0.0304	0.0166	0.2381	0.2916
	NMI	0.5460	0.9864	0.8705	0.3609	0.9893		NMI	0.0000	0.0000	0.0145	0.1635	0.3129
Dim2	Accuracy	0.8259	1.0000	0.9289	1.0000	1.0000	TumTyp	Accuracy	0.3483	0.9975	0.3059	0.9975	0.9975
	F-Score	0.8482	1.0000	0.9384	1.0000	1.0000		F-Score	0.5092	0.9976	0.2666	0.9976	0.9976
	ARI	0.7549	1.0000	0.8714	1.0000	1.0000		ARI	0.1445	0.9938	0.0025	0.9938	0.9938
	NMI	0.8782	1.0000	0.9337	1.0000	1.0000		NMI	0.2577	0.9898	0.0042	0.9898	0.9898
ShapeT	Accuracy	0.2667	0.8808	0.2799	1.0000	1.0000	DrivFace	Accuracy	0.3053	0.6436	0.2871	0.5924	0.6485
	F-Score	0.3600	0.9586	0.3732	1.0000	1.0000		F-Score	0.3685	0.7489	0.3303	0.5614	0.6853
	ARI	0.0910	0.7819	0.0938	1.0000	1.0000		ARI	0.2394	0.4684	0.0076	0.4701	0.3663
	NMI	0.0930	0.6104	0.0882	1.0000	1.0000		NMI	0.2727	0.4285	0.0138	0.5018	0.4604

Table 3: The results' comparison for different methods

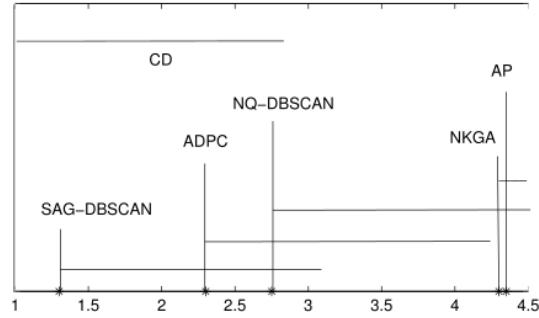


Figure 4: Critical difference (CD) diagram of the post-hoc Nemenyi test ($\alpha = 0.10$)

number of clusters (TABLE 2), than the other methods under comparison. Based on this work, it will be interesting to extend our method into a fully adaptive method in the future.

- [1] C. P. Kappe M. Böttinger H. Lette, Analysis of Decadal Climate Predictions with User guided Hierarchical Ensemble Clustering, Computer Graphics Forum, vol. 38, no. 3, pp. 505-515, Jul 2019.
- [2] T. Wang, J. Zhang, K. Huang, Generalized gene co-expression analysis via subspace clustering using low-rank representation, BMC Bioinformatics, 20 (Suppl 7): 196, DOI: 10.1186/s12859-019-2733-5, 2019.
- [3] A. Pessia, J. Corander, Kpax3: Bayesian bi-clustering of large sequence datasets, Bioinformatics, vol. 34, no. 12, pp. 2132-2133, Jun 2018.
- [4] J. D. Hamilton, "A new approach to the economic analysis of nonstationary time series and the business cycle," Econometrica vol., vol. 57, no. 2, pp. 357-384, Mar 1989.

- [5] G. Leibon, S. Pauls, D. Rockmore, R. Savell, "Topological structures in the equities market network," Proc. Natl. Acad. Sci. U.S.A., vol. 105, no. 52, pp. 20589-20594, Dec 2008.
- [6] S. Galbraith, J. A. Daniel, B. Vissel, "A study of clustered data and approaches to its analysis," J. Neurosci., vol. 30, no. 32, pp. 10601-10608, Aug 2010.
- [7] H. K. Aljobouri et al., Clustering fMRI data with a robust unsupervised learning algorithm for neuroscience data mining, J Neurosci Methods, vol. 299, pp. 45-54, Apr 2018.
- [8] A. Rodriguez, A. Laio, "Clustering by fast search and find of density peaks," Science, vol. 344, no. 6191, pp. 1492-1496, Jun 2014.
- [9] R. Mehmood et al, "Clustering by fast search and find of density peaks via heat diffusion," Neurocomputing, vol. 208, pp. 210-217, Oct 2016.
- [10] M. Ester, H.P. Kriegel, J. Sander, and X. Xu, "A density-based algorithm for discovering clusters in large spatial

- databases with noise,” *Data Mining Knowl. Discovery*, vol. 96, no. 34, pp. 226-231, Aug 1996.
- [11] Y. Chen, S. Tang, et al, “A fast clustering algorithm based on pruning unnecessary distance computations in DBSCAN for high-dimensional data,” *Pattern Recognition*, vol. 83, pp. 375-387, Nov 2018.
- [12] Y. Zhu, K. M. Ting, and M. J. Carman, “Grouping points by shared subspaces for effective subspace clustering,” *Pattern Recognition*, vol. 83, pp. 230-244, May 2018.
- [13] R. Agrawal, J. E. Gehrke, D. Gunopulos, and P. Raghavan, “Automatic subspace clustering of high dimensional data for data mining applications,” in *Proc. ACM SIGMOD Int. Conf. Manage. Data (SIGMOD)*, Seattle, WA, USA, pp. 94-105, Jun 1998.
- [14] C. Deng et al., Gridwave: a grid-based clustering algorithm for market transaction data based on spatial-temporal density-waves and synchronization, *Multimedia Tools and Applications*, vol. 77, no. 21, pp. 1-15, Jan 2018.
- [15] G. Sheikholeslami, S. Chatterjee, A. Zhang, “WaveCluster: a wavelet-based clustering approach for spatial data in very large data bases,” *VLDB J.*, vol. 8, pp. 289-304 Feb 2000.
- [16] K. Murphy, T. B. Murphy, Gaussian parsimonious clustering models with covariates and a noise component, *Advances in Data Analysis and Classification*, Sep 2019. DOI: 10.1007/s11634-019-00373-8.
- [17] A. O’Hagan et al., Investigation of Parameter Uncertainty in Clustering Using a Gaussian Mixture Model Via Jackknife, Bootstrap and Weighted Likelihood Bootstrap, *Computational statistics*, May 2019. DOI: 10.1007/s00180-019-00897-9.
- [18] T. Chen, N. L. Zhang, T. Liu, K. M. Poon, Y. Wang, “Model-based multidimensional clustering of categorical data,” *Artif. Intell.*, vol. 176, no. 1, pp. 2246-2269, Jan 2012.
- [19] J. MacQueen, “Some Methods for Classification and Analysis of Multivariate Observations,” in *Proceedings of the Fifth Berkeley Symposium on Mathematical Statistics and Probability*, L. M. Le Cam, J. Neyman, Eds. (Univ. California Press, Berkeley, CA), vol. 1, pp. 281-297, Jan 1967.
- [20] R. Zhang, X. Li et al., Deep Fuzzy K-Means with Adaptive Loss and Entropy Regularization, *IEEE Transactions on Fuzzy Systems*, Oct 2019. DOI: 10.1109/TFUZZ.2019.2945232.
- [21] R. Zhang et al., Joint Learning of Fuzzy k-Means and Non-negative Spectral Clustering With Side Information, *IEEE Transactions on Image Processing*, vol. 28, no. 5, pp. 2152-2162, 2019.
- [22] D. W. Choi, C. W. Chung, A K-partitioning algorithm for clustering large-scale spatio-textual data, *Information Systems*, vol. 64, pp. 1-11, Mar 2017.
- [23] K. Lahari, M. R. Murty, S. C. Satapathy, “Partition based clustering using genetic algorithm and teaching learning based optimization: performance analysis,” *Adv. Intell. Syst. Comput.*, vol. 338, pp. 191-200, Mar 2015.
- [24] J. Wang, W. Zheng, Y. Qian, J. Liang, A Seed Expansion Graph Clustering Method for Protein Complexes Detection in Protein Interaction Networks, *Molecules*, vol. 22, no. 12, pp. 1-19, Dec 2017. Doi:10.3390/molecules22122179.
- [25] P. Pipenbacher, A. Schliep, S. Schneckener et al, “ProClust: improved clustering of protein sequences with an extended graph-based approach,” *Bioinformatics*, vol. 18, no. 2, pp. 182-191, Jun 2002.
- [26] V. V. Vu, H. Q. Du, “Graph-based Clustering with Background Knowledge,” *SoICT 2017 Proceedings of the Eighth International Symposium on Information and Communication Technology*, NY, USA, pp. 167-172, Dec 2017.
- [27] T. Zhang, R. Ramakrishnan, and M. Livny, “BIRCH: An efficient data clustering method for very large databases,” in *Proc. ACM SIGMOD Int. Conf. Manage. Data (SIGMOD)*, Montreal, QC, Canada, vol. 25, no. 2, pp. 103-114, Jun 1996.
- [28] J. Das, S. Majumder, et al., Collaborative Recommendations using Hierarchical Clustering based on K-d Trees and Quadrees, *International Journal of Uncertainty Fuzziness and Knowledge-Based Systems*, vol. 27, no.4, pp. 637-668, Jun 2019.
- [29] G. Karypis, E. H. Han, and V. Kumar, “CHAMELEON: A hierarchical clustering algorithm using dynamic modeling,” *IEEE Computer*, vol. 32, no. 8, pp. 68-75, Aug 1999.
- [30] J. H. Kim et al., “AA-DBSCAN: an approximate adaptive DBSCAN for finding clusters with varying densities,” *J. Supercomput.*, vol. 75, pp. 142-169, May 2018.
- [31] A. Bryant, K. Bryant, “RNN-DBSCAN: A Density-Based Clustering Algorithm Using Reverse Nearest Neighbor Density Estimates,” *IEEE T. Knowl. Data En.*, vol. 30, no. 6, pp. 1109-1121, Jun 2018.
- [32] Y. Zhu, K. Ting, M. Carman, “Density-ratio based clustering for discovering clusters with varying densities,” *Pattern Recogn.*, vol. 60, pp. 983-997, Dec 2016.
- [33] D. Wu, D. L. Olson, Z. Y. Dong, Data mining and simulation: a grey relationship demonstration, *International Journal of Systems Science*, vol. 37, no. 13, pp. 981-986, Oct 2006.
- [34] H. H. Yang, J. L. Liu, M. C. S. Chang, J. C. Yang, Improvement of e-government service process via a grey relation agent mechanism, *Expert Systems with Applications*, vol. 39, no. 10, pp. 9755-9763, Aug 2012.
- [35] K. C. Chang, M. F. Yeh, Grey relational analysis based approach for data clustering, *IEE Proceedings-Vision Image and Signal Processing*, vol. 152, no. 2, pp. 165-172, Apr 2005.

- [36] C. H. Lin, C. H. Wu, P. Z. Huang, Grey clustering analysis for incipient fault diagnosis in oil-immersed transformers, *Expert Systems with Applications*, vol. 36, pp. 1371-1379, 2009.
- [37] X. Li, K. W. Hipel, Y. Dang, An improved grey relational analysis approach for panel data clustering, *Expert Systems With Applications*, vol. 42, pp. 9105-9116, 2015.
- [38] J. Deng, Introduction to grey system theory, *Journal of Grey System*, vol. 1, pp. 1-24 1989.
- [39] W. Feng, S. Hao, X. Feng, Z. Fan, Fault-tolerant federated filtering algorithm based on improved B-style grey relationship degree and balance coefficient, *Journal of Computer Applications*, vol. 32, no. 5, pp. 1307-1310, 2012.
- [40] Y. Chen, X. Hu et al, "Fast density peak clustering for large scale data based on kNN," *Knowledge-Based Systems*, Jul 2019. [Online]. Available: <https://doi.org/10.1016/j.knosys.2019.06.032>
- [41] M. Du, S. Ding, H. Jia, "Study on density peaks clustering based on k-nearest neighbors and principal component analysis," *Knowl. Based Syst.*, vol. 99, pp. 135-145, May 2016.
- [42] B. J. Frey, D. Dueck, "Clustering by passing messages between data points," *Science*, vol. 315, no. 5814, pp. 972-976, Feb 2007.
- [43] T. Liu, H. Li, X. Zhao, "Clustering by Search in Descending Order and Automatic Find of Density Peaks," *IEEE Access*, vol. 7, pp. 133772-133780, Sep 2019.
- [44] R. Tinós, L. Zhao, F. Chicano, D. Whitley, "NK Hybrid Genetic Algorithm for Clustering," *IEEE Transactions on Evolutionary Computation*, vol. 22, no. 5, pp. 748-761, Apr 2018.
- [45] C. J. Veenman, M. J. T. Reinders, E. Backer, "A maximum variance cluster algorithm" *IEEE Trans. Pattern Analysis and Machine Intelligence*, vol. 24, no. 9, pp. 1273-1280, Sep 2002.
- [46] P. Franti, O. Virtajoki, "Iterative shrinking method for clustering problems," *Pattern Recognit.*, vol. 39, no. 5, pp. 761-775, May 2006.
- [47] P. Franti, O. Virtajoki, V. Hautamaki, "Fast agglomerative clustering using a k-nearest neighbor graph," *IEEE Trans. Pattern Anal. Mach. Intell.*, vol. 28, no. 11, pp. 1875-1881, Nov 2006.
- [48] R. A. Fisher, "The use of multiple measurements in taxonomic problems," *Annual Eugenics*, vol. 7, no. 2, pp. 179-188, Sep 1936.
- [49] F. Huang, X. Li, S. Zhang, J. Zhang, "Harmonious Genetic Clustering," *IEEE Transactions On Cybernetics*, vol. 48, no. 1, pp. 199-214, Jan 2018.
- [50] J. G. Rohra et al, "User Localization in an Indoor Environment Using Fuzzy Hybrid of Particle Swarm Optimization & Gravitational Search Algorithm with Neural Networks," In *Proceedings of Sixth International Conference on Soft Computing for Problem Solving*, pp. 286-295, Feb 2017.
- [51] E. Berthonnaud et al, "Analysis of the sagittal balance of the spine and pelvis using shape and orientation parameters," *Journal of Spinal Disorders & Techniques*, vol. 18, no. 1, pp. 40-47, Feb 2005.
- [52] J. N. Weinstein et al. "The cancer genome atlas pan-cancer analysis project," *Nature genetics*, vol. 45 no. 10, pp. 1113-1120, 2013.
- [53] D. C. Katherine et al., "A reduced feature set for driver head pose estimation," *Applied Soft Computing*, Vol. 45, pp. 98-107, Aug 2016.
- [54] L. Du, Y. Pan, X. Luo, "Robust spectral clustering via matrix aggregation," *IEEE Access*, Vol. 6, pp. 53661-53670, Sep 2018.
- [55] S. Abbasi, S. Nejatian, et al., "Clustering ensemble selection considering quality and diversity," *Artif. Intell. Rev.*, vol. 52, pp. 1311-1340, Jan 2019.